PHYSICAL REVIEW B VOLUME 32, NUMBER 11 1 DECEMBER 1985

Scaling in an interacting two-component (valence-fluctuation) electron gas

C. M. Varma
AT&T Bell Laboratories, Murray Hill, New Jersey 07974

A. Zawadowski
Central Research Institute for Physics, H-1525, Budapest, POB 49 Hungary
(Received 17 June 1985)

A one-dimensional model of a two-component interacting electron gas with different Fermi wave vectors and Fermi velocities is considered. The method of the multiplicative renormalization group is used and the leading-order equations for the vertices as the frequency or momentum cutoff is reduced are derived. There are in general twelve different vertices in which there are logarithmic corrections in scaling, which may be broadly classified as intracomponent interactions, intercomponent exchange interactions, and charge-transfer interactions. The scaling equations are numerically solved in a limited regime appropriate for the valence-fluctuation problem. We discover that intercomponent charge-fluctuation interactions do not affect the dominant instabilities which are primarily determined by the intercomponent exchange interactions (provided intracomponent channels by themselves are stable, as in the range of parameters examined). The theoretical connection of the fluctuating-valence problem to the Kondo-like problems which is phenomenologically observed is thereby established.

I. INTRODUCTION

The one-component interacting electron gas in one dimension has been studied exhaustively by a variety of methods.[1] The Fermi-liquid properties and the instabilities—charge-density waves and various forms of magnetism and superconductivity—have been mapped out in the various regimes of relevant parameters. This has in turn shed considerable insight into the properties of actual materials, both pseudo-one-dimensional and two or three dimensional. In this paper we study the properties of a two-component interacting electron gas in one dimension, with the ratio of the mass of the two components, in general, different from one. Because the number of competing interactions is much larger, the problem has a much richer structure than that of the one-component problem. The problem occurs in solid-state physics in a wide variety of contexts—in transition metals and in rare-earth metals and in their compounds. A strong motivation for our work is the properties of the so-called fluctuating-valence (also called mixed-valence or intermediate-valence) compounds.

A. Valence fluctuations

The fluctuating-valence[2] problem arises in rare-earth and the actinide compounds, when the chemical potential is *pinned* by the $4f$ or the $5f$ resonances whose eigenvectors in the isolated atoms correspond to very localized orbitals. This occurs in only about 10% of the cases. About 90% of the cases belong in the localized-moment regime. The Coulomb repulsion energy for electrons in the localized orbitals is large, of the order 10 eV and their hybridization with the conduction bands very weak, so that when the partially (but integrally) occupied resonances lie *well below* the chemical potential, they have negligible charge (valence) fluctuations and carry localized magnetic moments. The scattering and polarization of the conduction electrons in this situation is very weak and leads to Ruderman-Kittel-Kasuya-Yosida (RKKY) coupling between the moments and long-range magnetic order of these moments at low temperatures. By contrast, in the fluctuating-valence regime, a high-temperature regime of Curie-Weiss susceptibility characteristic of localized moments, gives way at low temperature to a temperature-independent (Pauli) susceptibility characteristic of itinerant electrons. The value of this susceptibility is very large. The specific heat at low temperatures varies linearly with temperature, also characteristic of itinerant electrons. The magnitude of the specific heat and the susceptibility suggest that the ground state and the low-lying excitations are characteristic of a Fermi liquid with an effective mass m^*/m of order 10^2 and not very significant exchange enhancement in a majority of the cases. Only one fluctuating-valence compound, TmSe (and its alloys), is known[3] to undergo a magnetic phase transition. This is a special situation[4] arising when both the valence states of the ion carry a magnetic moment. In all other clearly defined cases one of the valence states carries no moment.

If the Fermi level is pinned by the f resonance, it follows that f orbitals undergo charge fluctuations. Phenomenologically, there appears to be a third class of compounds,[5,6] in which the f resonance is below but not too far below the chemical potential. The relevant energy scale would appear to be the resonance width $\Gamma \simeq \pi V^2 \rho(0)$, where V is the appropriate hybridization matrix element of f orbitals with conduction electrons whose density of

states at the Fermi level is $\rho(0)$. In this case, charge fluctuations should be negligible. They also behave as Fermi liquids, with an even large mass of $O(10^3)$. The considerations in this paper are confined to a situation in which there are explicit charge fluctuations in the f orbitals but the close connection between the two problems will be apparent.

So far the properties only of an isolated fluctuating-valence impurity[7] in a conduction band are well understood and some work has been done for the interaction[8] between a pair of such impurities. The isolated impurity plus the conduction band, despite the charge fluctuations, has a singlet ground state, just like the Kondo impurity.[9] The theoretical problem in the fluctuating-valence lattice is to understand how, despite the strong interactions, the lattice has a singlet ground state with low-lying excitations characteristic of Fermi liquids.

B. Fermi liquids

In a system of interacting fermions, a Fermi-liquid ground state may be looked upon as a weak-coupling fixed point in the sense that at low energies the various interaction vertices scale to constants—the Landau parameters, and the discontinuity at the Fermi surface is preserved. It appears that a different kind of Fermi liquid is possible, where the scaling is to strong coupling and a new type of ground state is organized at $T\rightarrow 0$, the excitations about which are of fermionic nature. The single-impurity Kondo effect is the simplest manifestation of this possibility—the fluctuating-valence solids and the so-called heavy fermion solids may be others.

We will employ the method of the multiplicative renormalization group to study the problem. We will also confine our detailed attention to a one-dimensional model, as all the divergent terms in one dimension can be summed up by the renormalization-group method. If the unrenormalized interactions are such that scaling is to the weak-coupling fixed point, this method leads to the correct qualitative results in the leading order. If in one dimension the problem scales to weak coupling, the results are likely to be valid in three dimensions. If for some choice of interactions some of the vertices scale to strong coupling the present method is inadequate for determining the ground state and the low-lying excitations. The manner of scaling to strong coupling can be very instructive, however, for understanding the physics of the problem. There are, in general, 12 different kinds of interactions with infrared divergent corrections in perturbation theory. These are outlined in Sec. II. Broadly, these are interactions in which all incoming and outgoing particles are of the same type and those in which they are different. The latter are of two kinds, which may be described somewhat imprecisely as charge-fluctuation interactions from one type to another and exchange interactions between the two types. The problem therefore has interactions which appear in the one-component electron gas, the single-impurity Kondo problem, and the single-impurity fluctuating-valence problem. These various interaction channels interfere and, from an examination of the most divergent channel, one can draw important conclusions even if the flows are to strong coupling.

II. THE MODEL

A. Kinetic energy

We consider a model which has two types of electrons labeled A and B, respectively. The B electrons can hop to their neighbors with transfer integrals t; the A orbitals have a weak hybridization. Whether the hybridization is on site or at neighboring sites with the B orbitals is not relevant in our treatment. Both A and B orbitals are considered nondegenerate. Extensions of the method used here for the degenerate case are straightforward. In that case A would denote the f orbitals and B the s and d orbitals. The kinetic energy operator is therefore

$$H_0' = \epsilon_A \sum_{i,\sigma} a_{i\sigma}'^{\dagger} a_{i\sigma}' + \sum_{i<j,\sigma} t_{ij}(b_{i\sigma}'^{\dagger} b_{j\sigma}' + \text{c.c.}) + V\sum_{i,\sigma}(a_{i\sigma}'^{\dagger} b_{i\sigma}' + \text{c.c.}), \quad V \ll \text{typical } t_{ij} . \tag{1}$$

The reason for putting the prime in various quantities in Eq. (1) will be clear momentarily. The largest interactions in the problem are those between electrons on the same site in the A orbitals. Usually the other interactions are neglected to begin with, but since they are generated in higher-order perturbation theory, we might as well start with the general problem and consider all possible vertices. These will be generally of two kinds, those that lead to singular (logarithmic) corrections in perturbation theory and those that lead to nonsingular contributions. The renormalization group is well suited to considering the former and they will be classified in the next section. H_0, Eq. (1), is trivially diagonalizable. We assume that we can group the leading effect of the second type of vertices (i.e., the self-energy corrections due to them) together with H_0 to give an effective one-electron Hamiltonian. This will describe two bands, which in general, in one dimension, will have two sets of Fermi vectors $\pm k_A$ and $\pm k_B$:

$$H_0 \simeq \sum_k \epsilon_{kA} a_{k\sigma}^{\dagger} a_{k\sigma} + \epsilon_{kB} b_{k\sigma}^{\dagger} b_{k\sigma} . \tag{2}$$

The original orbitals, i.e., a' and b' of (1) get mixed up, but the bandwidth W_A of the $\epsilon_{kA} \ll W_B$, the bandwidth of ϵ_{kB} which is given in terms of the t in Eq. (1). The electron velocity $\partial\epsilon_{kA}/\partial k$ is much smaller than $\partial\epsilon_{kB}/\partial k$ near the Fermi surface. We will work only with $k_A \neq k_B$, otherwise a semiconducting situation will arise, which we do not wish to treat. We will also ignore any gaps in ϵ_{kA} and ϵ_{kB}.

In these simplifications the principal shortcoming is that we are considering a one-dimensional problem. Ignoring the small gaps away from the Fermi surface is not a crucial shortcoming because the momentum range of the hybridization is negligible compared to the momentum cutoff k_C.

B. Interactions

As discussed in the preceding section, two electron bands are considered with two essentially different Fermi momenta which are labeled as k_A and k_B. The corresponding electron creation operators are $a_{ks}^{\dagger}$ and $b_{ks}^{\dagger}$, respectively, where s stands for the spin. Thus, the unper-

turbated Hamiltonian with linearized dispersion is the following:

$$H_0=\sum_{k,s}(k-k_A)v_A a_{ks}^{\dagger}a_{ks}+\sum_{k,s}(-k-k_A)v_A a_{ks}^{\dagger}a_{ks}+\sum_{k,s}(k-k_B)v_b b_{ks}^{\dagger}b_{ks}+\sum_{k,s}(-k-k_B)v_B b_{ks}^{\dagger}b_{ks}\ . \tag{3}$$

The momentum summations are restricted to regions which are symmetrically placed around the Fermi momenta, and the momentum cutoff k_C is applied for momenta measured from the Fermi momenta (see Fig. 1). As discussed, it is assumed, furthermore, that these linearized spectra are approximations of a realistic dispersion curve where hybridization effects and effects of nonsingular perturbations have already been taken into account.

The electron-electron interaction will be considered in logarithmic approximation, thus the logarithmically singular terms will be kept which arise from the region of the Fermi energy. There are, however, nonlogarithmic contributions as well. The scheme to be followed is to consider only those vertices which contribute to logarithmic terms, and all of the nonlogarithmic vertex and self-energy renormalization are assumed to be contained in the starting vertices and Fermi velocities. Thus, vertices do not occur which have, e.g., three A-particle and one B-particle legs; as due to momentum conservation, at least one particle has energy far from the Fermi energy.

The vertices are labeled in a way depicted in Fig. 2, where the first and last indices correspond always to particles with the same spin. The signs associated with the number of closed loops in the diagrams will be determined with this convention. Following the notation generally accepted, $\Gamma^{\parallel}$ corresponds to the scattering of two particles with parallel spins and $\Gamma^{\perp}$ to particles with opposite spins. Furthermore, for the sake of simplicity the initial vertices depend on whether the electrons belong to the branches A or B and to the left or right part of the dispersion curve, but are independent of the particular values of the momenta inside those regions. In this way the vertices can be labeled, e.g., as $\Gamma^{\perp}_{A^+B^-B^-A^+}$, etc., where the A^+ means the A particle with momentum on the right-hand part of the dispersion curve, etc. As in the case of a single-band model, the scattering processes in which all the particles are on the left- or right-hand side of the dispersion curves do not contribute in the logarithmic approximations. Thus, the two incoming and the two outgoing particles are always on opposite sides of the dispersion curve. A scattering will be labeled by a superscript (1) if the particles associated with the first and last indices are on the opposite sides, and by (2) if those are on the same side. In this way a vertex $\Gamma^{\perp}_{A^+A^-B^+B^-}=\Gamma^{\perp(1)}_{AABB}$ and $\Gamma^{\perp}_{A^+A^-B^-B^+}=\Gamma^{\perp(2)}_{AABB}$, etc. Finally, for parallel spins the identity $\Gamma^{\parallel(1)}_{abcd}=-\Gamma^{\parallel(2)}_{abdc}$ holds; thus, only one of these quantities will be kept, namely, $\Gamma^{\parallel(1)}_{abcd}=\Gamma^{\parallel}_{abcd}$, where the index (1) will be dropped in the parallel spins channel for the sake of brevity.

Using these notations the following twelve vertices must be introduced:

$$\begin{aligned}&\Gamma^{\perp(1)}_{AABB},\ \Gamma^{\perp(2)}_{AABB},\ \Gamma^{\parallel}_{AABB}\ ,\\ &\Gamma^{\perp(1)}_{ABAB},\ \Gamma^{\perp(2)}_{ABBA},\ \Gamma^{\parallel}_{ABAB}\ ,\\ &\Gamma^{\perp(1)}_{AAAA},\ \Gamma^{\perp(2)}_{AAAA},\ \Gamma^{\parallel}_{AAAA}\ ,\\ &\Gamma^{\perp(1)}_{BBBB},\ \Gamma^{\perp(2)}_{BBBB},\ \Gamma^{\parallel}_{BBBB}\ .\end{aligned} \tag{4}$$

The interchange of the incoming lines by the outgoing lines does not lead to new couplings.

These interactions may arise from Coulomb interactions or electron-phonon interactions, or from these in combination with the hybridization V between the a' and b' orbitals of Eq. (1). In the usual model Hamiltonians used for the valence-fluctuation problem, only a large Coulomb repulsion between the electrons with different spins in the a' orbital on the same site is added to Eq. (1). This may be associated with Γ_{AAAA}. The hybridization V produces in second-order perturbation theory an exchange interaction J between a' and b' orbitals, when the effect of U is included. J may be associated with Γ_{ABAB} as may direct Coulomb or electron-phonon—induced interactions.

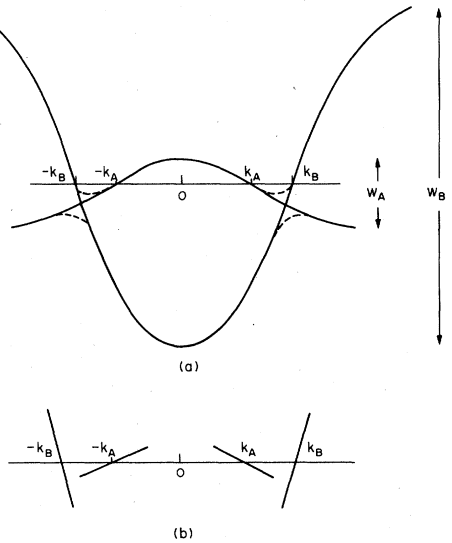

FIG. 1. Kinetic energy dispersion for the two components A and B is shown. The dispersion of A is shown inverted with respect to B, but this is not essential. In (a) the dashed lines represent the effect of hybridization. In (b) the idealized (linearized) dispersion is depicted. All branches cover a momentum region of width $2k_C$ where k_C is the cutoff.

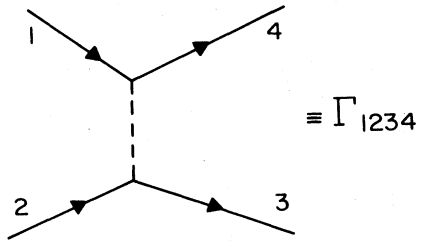

FIG. 2. Illustrates the labeling of the vertices as described in the text.

The *ABAB* channel is what appears in the single-impurity Kondo problem and will play a major role in the present problem. The *AABB* channel transfers electrons between the *A* and *B* components and may be looked upon as a charge-fluctuation channel.

The unrenormalized Green's functions $G^{(0)}_{A^{\pm}}$ and $G^{(0)}_{B^{\pm}}$ have the following form:

$$G^{(0)}_{A^{\pm}{}_{,s}}(k,\omega)=\frac{1}{\omega-(\pm k-k_A)v_A}$$

and (5)

$$G^{(0)}_{B^{\pm}{}_{,s}}(k,\omega)=\frac{1}{\omega-(\pm k-k_B)v_B}\ ,$$

where ω is the energy.

In the logarithmic approximation the basic skeleton diagrams are bubbles with two parallel or antiparallel lines which can be either *AA*, *BB*, or *AB* propagators. These diagrams have the multiplicative factor $(2v_A)^{-1}$, $(2v_B)^{-1}$, and $(v_A+v_B)^{-1}$, respectively, which are due to density of states. In the following, dimensionless vertex couplings will be used:

$$\frac{1}{\pi}\frac{1}{v_A+v_B}\Gamma\rightarrow\Gamma\ .$$

The factor $(v_A+v_B)^{-1}$ is produced in the *AB* channel; thus, in the *AA* or *BB* channels a dimensionless correction factor

$$\alpha=\frac{v_A+v_B}{2v_A}\ \text{and}\ \beta=\frac{v_A+v_B}{2v_B} \tag{6}$$

must be taken into account. As it has been assumed that $v_B\gg v_A$, thus, $\alpha\gg 1$ and $\beta\sim\frac{1}{2}$.

A typical diagram shown in Fig. 3 has the contribution

$$-i\int\frac{dk'}{2\pi}\int\frac{d\omega}{2\pi}G_{A^+}(k',\omega')G_{B^-}(-k'+k_A-k_B,\omega-\omega')$$
$$=\frac{1}{\pi(v_A+v_B)}\ln\frac{(v_A+v_B)k_C}{\omega}\ ,$$

where the imaginary part is dropped, as it does not contribute in the leading logarithmic approximation. In the *AA* and *BB* channel, $\ln(2v_Ak_C/\omega)$ and $\ln(2v_Bk_C/\omega)$ occur. Keeping only the singular term in ω, all the logarithmic terms can be replaced by $\ln[(v_A+v_B)k_C/\omega]$ and the variable $(v_A+v_B)k_C/\omega=S$ will be the only relevant one.

III. SCALING

The renormalization group is generated by reducing the momentum cutoff k_C in small steps. For the description of the method we refer to Sólyom's review article.[1] We only quote those final results, which are generated through summing appropriate second-order diagrams and then using the Lie equations. As an example, the diagrams summed for the $\Gamma^{\perp(1)}_{AABB}$ vertex are depicted in Fig. 4, and lead to Eq. (7a). Equations (7b) to (7l) are similarly obtained:

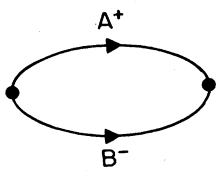

FIG. 3. A typical diagram contributing in the leading logarithmic approximation as discussed in the text.

$$S\frac{\partial\tilde{\Gamma}^{\perp(1)}_{AABB}}{\partial S}=(\alpha\tilde{\Gamma}^{\perp(2)}_{AAAA}+\beta\tilde{\Gamma}^{\perp(2)}_{BBBB})\tilde{\Gamma}^{\perp(1)}_{AABB}$$
$$+(\alpha\tilde{\Gamma}^{\perp(1)}_{AAAA}+\beta\tilde{\Gamma}^{\perp(1)}_{BBBB})\tilde{\Gamma}^{\perp(2)}_{AABB}$$
$$+2\tilde{\Gamma}^{\perp(1)}_{ABAB}\tilde{\Gamma}^{\parallel}_{AABB}+2\tilde{\Gamma}^{\perp(1)}_{AABB}\tilde{\Gamma}^{\parallel}_{ABAB}\ , \tag{7a}$$

$$S\frac{\partial\tilde{\Gamma}^{\perp(2)}_{AABB}}{\partial S}=\alpha\tilde{\Gamma}^{\perp(2)}_{AAAA}\tilde{\Gamma}^{\perp(2)}_{AABB}+\beta\tilde{\Gamma}^{\perp(2)}_{BBBB}\tilde{\Gamma}^{\perp(2)}_{AABB}$$
$$+\alpha\tilde{\Gamma}^{\perp(1)}_{AAAA}\tilde{\Gamma}^{\perp(1)}_{AABB}+\beta\tilde{\Gamma}^{\perp(1)}_{BBBB}\tilde{\Gamma}^{\perp(1)}_{AABB}$$
$$-2\tilde{\Gamma}^{\perp(2)}_{ABBA}\tilde{\Gamma}^{\perp(2)}_{AABB}\ , \tag{7b}$$

$$S\frac{\partial\tilde{\Gamma}^{\perp(1)}_{ABAB}}{\partial S}=2\tilde{\Gamma}^{\perp(2)}_{ABBA}\tilde{\Gamma}^{\perp(1)}_{ABAB}+2\tilde{\Gamma}^{\parallel}_{ABAB}\tilde{\Gamma}^{\perp(1)}_{ABAB}$$
$$+2\tilde{\Gamma}^{\parallel}_{AABB}\tilde{\Gamma}^{\perp(1)}_{AABB}\ , \tag{7c}$$

$$S\frac{\partial\tilde{\Gamma}^{\perp(2)}_{ABBA}}{\partial S}=(\Gamma^{\perp(1)}_{ABAB})^2-(\tilde{\Gamma}^{\perp(2)}_{AABB})^2\ , \tag{7d}$$

$$S\frac{\partial\tilde{\Gamma}^{\perp(1)}_{AAAA}}{\partial S}=2\alpha\tilde{\Gamma}^{\perp(2)}_{AAAA}\tilde{\Gamma}^{\perp(1)}_{AAAA}+2\beta\tilde{\Gamma}^{\perp(2)}_{AABB}\tilde{\Gamma}^{\perp(1)}_{AABB}$$
$$+2\alpha\tilde{\Gamma}^{\parallel}_{AAAA}\tilde{\Gamma}^{\perp(1)}_{AAAA}\ , \tag{7e}$$

$$S\frac{\partial\tilde{\Gamma}^{\perp(1)}_{BBBB}}{\partial S}=2\beta\tilde{\Gamma}^{\perp(2)}_{BBBB}\tilde{\Gamma}^{\perp(1)}_{BBBB}+2\alpha\tilde{\Gamma}^{\perp(2)}_{AABB}\tilde{\Gamma}^{\perp(1)}_{AABB}$$
$$+2\beta\tilde{\Gamma}^{\parallel}_{BBBB}\tilde{\Gamma}^{\perp(1)}_{BBBB}\ , \tag{7f}$$

$$S\frac{\tilde{\Gamma}^{\perp(2)}_{AAAA}}{\partial S}=\alpha(\tilde{\Gamma}^{\perp(1)}_{AAAA})^2+\beta(\tilde{\Gamma}^{\perp(2)}_{AABB})^2+\beta(\tilde{\Gamma}^{\perp(1)}_{AABB})^2\ , \tag{7g}$$

$$S\frac{\partial\tilde{\Gamma}^{\perp(2)}_{BBBB}}{\partial S}=\beta(\tilde{\Gamma}^{\perp(1)}_{BBBB})^2+\alpha(\tilde{\Gamma}^{\perp(2)}_{AABB})^2+\alpha(\tilde{\Gamma}^{\perp(1)}_{AABB})^2\ , \tag{7h}$$

$$S\frac{\partial\tilde{\Gamma}^{\parallel}_{AABB}}{\partial S}=-(\alpha\tilde{\Gamma}^{\parallel}_{AAAA}+\beta\tilde{\Gamma}^{\parallel}_{BBBB})\tilde{\Gamma}^{\parallel}_{AABB}$$
$$+2\tilde{\Gamma}^{\parallel}_{AABB}\tilde{\Gamma}^{\parallel}_{ABAB}+2\tilde{\Gamma}^{\perp(1)}_{AABB}\tilde{\Gamma}^{\perp(1)}_{ABAB}\ , \tag{7i}$$

$$S\frac{\partial\tilde{\Gamma}^{\parallel}_{ABAB}}{\partial S}=(\tilde{\Gamma}^{\perp(1)}_{ABAB})^2+(\tilde{\Gamma}^{\parallel}_{AABB})^2+(\tilde{\Gamma}^{\perp(1)}_{AABB})^2\ , \tag{7j}$$

$$S\frac{\partial\tilde{\Gamma}^{\parallel}_{AAAA}}{\partial S}=\alpha(\tilde{\Gamma}^{\perp(1)}_{AAAA})^2-\beta(\tilde{\Gamma}^{\parallel}_{AABB})^2\ , \tag{7k}$$

$$S\frac{\partial\tilde{\Gamma}^{\parallel}_{BBBB}}{\partial S}=\beta(\tilde{\Gamma}^{\perp(1)}_{BBBB})^2-\alpha(\tilde{\Gamma}^{\parallel}_{AABB})^2\ . \tag{7l}$$

These equations must be solved with the boundary condi-

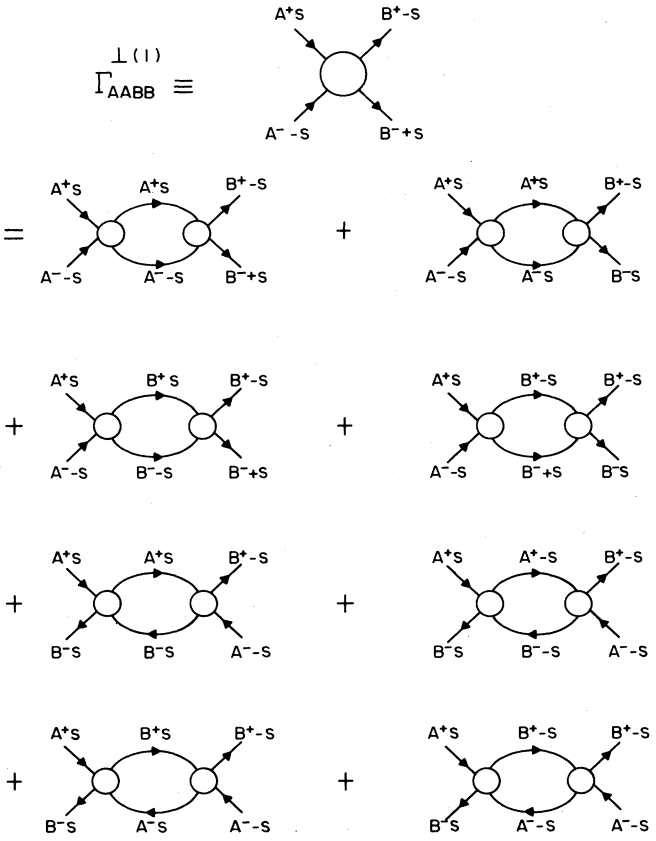

FIG. 4. Diagrams contributing the leading logarithmic corrections to the $\Gamma^{\perp(1)}_{AABB}$ vertex are shown as an example of how Eqs. (7) in the text are obtained.

tion that the vertices $\Gamma(S)\,|_{S=1}$ at $S=1$ are equal to their bare value. The bare value here means the vertices renormalized by only those processes which do not lead to any infrared divergences. This system of equations contains ten different equations, as it can be shown that the following two quantities are scale invariants:

$$(\Gamma^{\parallel}_{AAAA}+\beta\Gamma^{\parallel}_{ABAB})-(\Gamma^{\perp(2)}_{AAAA}+\beta\Gamma^{\perp(2)}_{ABBA})=\text{const}\ , \tag{8}$$

$$(\Gamma^{\parallel}_{BBBB}+\alpha\Gamma^{\parallel}_{ABAB})-(\Gamma^{\perp(2)}_{BBBB}+\alpha\Gamma^{\perp(2)}_{ABBA})=\text{const}\ . \tag{9}$$

In general, the only statement that can be made is that the derivatives of the following nine quantities are positive:

$$\frac{\partial\Gamma^{\perp(2)}_{AAAA}}{\partial S}>0\ , \tag{10a}$$

$$\frac{\partial\Gamma^{\perp(2)}_{BBBB}}{\partial S}>0\ , \tag{10b}$$

$$\frac{\partial\Gamma^{\parallel}_{ABAB}}{\partial S}>0\ , \tag{10c}$$

$$\frac{\partial\Gamma^{\perp(2)}_{AAAA}}{\partial S}+\beta\frac{\partial\Gamma^{\perp(2)}_{ABBA}}{\partial S}>0\ , \tag{10d}$$

$$\frac{\partial\Gamma^{\parallel}_{AAAA}}{\partial S}+\beta\frac{\partial\Gamma^{\parallel}_{ABAB}}{\partial S}>0\ , \tag{10e}$$

$$\frac{\partial\Gamma^{\perp(2)}_{AAAA}}{\partial S}-\frac{\partial\Gamma^{\parallel}_{AAAA}}{\partial S}>0\ , \tag{10f}$$

$$\frac{\partial\Gamma^{\perp(2)}_{BBBB}}{\partial S}+\alpha\frac{\partial\Gamma^{\perp(2)}_{ABBA}}{\partial S}>0\ , \tag{10g}$$

$$\frac{\partial\Gamma^{\parallel}_{BBBB}}{\partial S}+\alpha\frac{\partial\Gamma^{\parallel}_{ABAB}}{\partial S}>0\ , \tag{10h}$$

$$\frac{\partial\Gamma^{\perp(2)}_{BBBB}}{\partial S}-\frac{\partial\Gamma^{\parallel}_{BBBB}}{\partial S}>0\ . \tag{10i}$$

These inequalities imply that such quantities decrease in the scaling process as the cutoff k_C is reduced, thereby decreasing S.

A third of the vertices introduced above can be eliminated by assuming that the interaction is rotationally invariant in spin space; for instance, no spin-orbit coupling is allowed. In this case the interaction in an arbitrary channel can be given as

$$\Gamma^{\perp(1)}=g^{(1)},\quad \Gamma^{\parallel}=g^{(1)}-g^{(2)},\quad \Gamma^{\perp(2)}=g^{(2)}\ , \tag{11}$$

where in particular $\Gamma^{\parallel}_{ABAB}=g^{(1)}_{ABAB}-g^{(2)}_{ABBA}$.

Using this notation the Eqs. (7a)—(7l) are reduced to the following eight:

$$S\frac{\partial g^{(1)}_{AABB}}{\partial S}=(\alpha g^{(2)}_{AAAA}+\beta g^{(2)}_{BBBB})g^{(1)}_{AABB}$$
$$+(\alpha g^{(1)}_{AAAA}+\beta g^{(1)}_{BBBB})g^{(2)}_{AABB}+4g^{(1)}_{ABAB}g^{(1)}_{AABB}$$
$$-2(g^{(1)}_{ABAB}g^{(2)}_{AABB}+g^{(2)}_{ABBA}g^{(1)}_{AABB})\ , \tag{12a}$$

$$S\frac{\partial g^{(2)}_{AABB}}{\partial S}=\alpha g^{(2)}_{AAAA}g^{(2)}_{AABB}+\beta g^{(2)}_{BBBB}g^{(2)}_{AABB}+\alpha g^{(1)}_{AAAA}g^{(1)}_{AABB}$$
$$+\beta g^{(1)}_{BBBB}g^{(1)}_{AABB}-2g^{(2)}_{ABBA}g^{(2)}_{AABB}\ , \tag{12b}$$

$$S\frac{\partial g^{(1)}_{AAAA}}{\partial S}=2\alpha(g^{(1)}_{AAAA})^2+2\beta g^{(2)}_{AABB}g^{(1)}_{AABB}\ , \tag{12c}$$

$$S\frac{\partial g^{(2)}_{AAAA}}{\partial S}=\alpha(g^{(1)}_{AAAA})^2+\beta(g^{(2)}_{AABB})^2+\beta(g^{(1)}_{AABB})^2\ , \tag{12d}$$

$$S\frac{\partial g^{(1)}_{BBBB}}{\partial S}=2\beta(g^{(1)}_{BBBB})^2+2\alpha g^{(2)}_{AABB}g^{(1)}_{AABB}\ , \tag{12e}$$

$$S\frac{\partial g^{(2)}_{BBBB}}{\partial S}=\beta(g^{(1)}_{BBBB})^2+\alpha(g^{(2)}_{AABB})^2+\alpha(g^{(1)}_{AABB})^2\ , \tag{12f}$$

$$S\frac{\partial g^{(1)}_{ABAB}}{\partial S}=2(g^{(1)}_{AABB})^2-2g^{(2)}_{AABB}g^{(1)}_{AABB}+2(g^{(1)}_{ABAB})^2\ , \tag{12g}$$

$$S\frac{\partial g^{(2)}_{ABBA}}{\partial S}=(g^{(1)}_{ABAB})^2-(g^{(2)}_{AABB})^2\ , \tag{12h}$$

and the two scaling invariants are

$$g^{(1)}_{AAAA}-2g^{(2)}_{AAAA}+\beta(g^{(1)}_{ABAB}-2g^{(2)}_{ABBA})=C_1 \tag{13a}$$

and

$$g^{(1)}_{BBBB}-2g^{(2)}_{BBBB}+\alpha(g^{(1)}_{ABAB}-2g^{(2)}_{ABBA})=C_2\ . \tag{13b}$$

These equations reduce to the equations given by Menyhárd and Sólyom[10] if only one channel is considered. It is interesting to note that the $ABAB$ ($ABBA$) channel is connected only with the $AABB$ channel in a direct way. Furthermore, if $\alpha \gg 1$ and only the terms proportional to α are kept on the right-hand sides of the scaling equations, then the $ABAB$ channel does not enter in the scalings of the other channels.

The scaled coupling strengths obtained by the scaling equations can be used to analyze the renormalization and possible divergences of the different susceptibilities. In a model of one-dimensional metal with a single electron band there are four different susceptibilities which may diverge for some ranges of the initial coupling strengths: Peierls and spin-density susceptibilities and Cooper susceptibilities with spin singlet and spin triplet. In the present model all of these can be interpreted with only A or only B particles and also with a combination of A and B particles. In the latter channels the typical operators appearing in the susceptibilities are the following:

$$\sum_{s,\,|\kappa|<k_C} a^{\dagger}_{\kappa\pm k_A,s} b_{\kappa\pm k_B,s}, \quad \sum_{|\kappa|<k_C} a_{\kappa\pm k_A,\uparrow} b_{\kappa\pm k_B,\downarrow} ,$$
$$\sum_{s,\,|\kappa|<k_C} a^{\dagger}_{\kappa+k_A,s} b_{-\kappa-k_B,-s}, \quad \sum_{s,\,|\kappa|<k_C} a^{\dagger}_{\kappa+k_A,s} b_{-\kappa-k_B,s} . \tag{14}$$

The charge and spin densities are characterized by the wave vectors $\pm 2k_A$, $\pm 2k_B$, and $\pm(k_A+k_B)$ in the A, B, and in the combined AB channels, respectively. The most unusual ones are the Cooper pairs in the AB channel, as they are defined with finite momenta $\pm(k_A-k_B)$. The susceptibilities will be denoted as N_{ij}, $\chi_{ij}\Delta_{s,ij}$, and $\Delta_{t,ij}$, where the channel indices i and j are A or B. The quantities which obey simple scaling equations are defined as[1]

$$\begin{aligned}
\bar{N}_{ij}(s) &= \frac{\pi}{2}(v_i+v_j)\frac{\partial N_{ij}(s)}{\partial s} , \\
\bar{\chi}_{ij}(s) &= \frac{\pi}{2}(v_i+v_j)\frac{\partial \chi_{ij}(s)}{\partial s} , \\
\bar{\Delta}_{s,ij}(s) &= \frac{\pi}{2}(v_i+v_j)\frac{\partial \Delta_{s,ij}(s)}{\partial s} , \\
\bar{\Delta}_{t,ij}(s) &= \frac{\pi}{2}(v_i+v_j)\frac{\partial \Delta_{t,ij}(s)}{\partial s} ,
\end{aligned} \tag{15}$$

where, e.g., v_i is the Fermi velocity for the band $i=A,B$.

In the leading logarithmic approximation the scaling equations can be obtained in a straightforward way:

$$\frac{\partial \ln \bar{N}_{ij}(s)}{\partial \ln s} = \theta_{ij}(\Gamma^{\perp(1)}_{ijij} + \Gamma^{\parallel(1)}_{ijij}) \rightarrow \theta_{ij}(2g^{(1)}_{ijij} - g^{(2)}_{ijij}) , \tag{16a}$$

$$\frac{\partial \ln \bar{\chi}_{ij}(s)}{\partial \ln s} = -\theta_{ij}\Gamma^{\perp(2)}_{ijij} \rightarrow -\theta_{ij} g^{(2)}_{ijij} , \tag{16b}$$

$$\frac{\partial \ln \bar{\Delta}_{s,ij}}{\partial \ln s} = \theta_{ij}(\Gamma^{\perp(1)}_{ijij} + \Gamma^{\perp(2)}_{ijji}) \rightarrow \theta_{ij}(g^{(1)}_{ijij} + g^{(2)}_{ijji}) , \tag{16c}$$

$$\frac{\partial \ln \bar{\Delta}_{t,ij}(s)}{\partial \ln s} = -\theta_{ij}\Gamma^{\parallel}_{ijij} \rightarrow \theta_{ij}(g^{(1)}_{ijij} + g^{(2)}_{ijji}) , \tag{16d}$$

where the arrows point to the results for the rotational invariant special case given by Eq. (11). The proportionality factor θ_{ij} is $\alpha, 1, \beta$ in channels AA, AB, and BB, respectively.

IV. ANALYSIS OF THE SCALING EQUATIONS AND DISCUSSION

We first recall the results of the lowest-order multiplicative renormalization calculation for the one-component model.[1] In this, only the interactions $g^{(1)}_{AAAA}$ and $g^{(2)}_{AAAA}$ exist, and since $g^{(1)}_{AAAA} - 2g^{(2)}_{AAAA}$ is a constant, there is only one differential equation to study. The scaling trajectories satisfy $(g^{(1)})^2 - (g^{(2)})^2 = \text{const} \equiv C_0$. For $C_0 > 0$, the problem scales to weak coupling with $g^{(1)}$ and $g^{(2)}$ scaling to numbers, and the lowest-order results are qualitatively correct. For $C_0 < 0$, the problem scales to strong coupling and the method breaks down. Response functions have also been studied for this model. For $g^{(1)} < 0$, the charge-density wave response, N at $2k_F$ diverges (Peierls distortion) as well as the singlet superconducting response Δ_s. For $g^{(1)} > 0$ and $g^{(1)} - 2g^{(2)} < 0$, spin-density wave response χ at $2k_F$ diverges; while for $g^{(1)} > 0$, $g^{(1)} - 2g^{(2)} > 0$, both the singlet and the triplet superconducting response Δ_s and Δ_t diverge, of which the triplet has the stronger divergence. Monte Carlo calculations[11] on the same model confirm the qualitative validity of this phase diagram for $g^{(1)} > 0$.

A. The large-α approximation

In our problem, there are six coupled differential equations to analyze. This is, in general, possible only numerically. The structure of the equations is such that the properties can be studied analytically for $\alpha \gg 1$. It is discovered through a numerical analysis of the equations, however, that the region of validity of such analytic results is confined to the high-energy regime from the upper cutoff W_B to a fraction, depending upon the initial value of $g^{(1)}_{AABB}/g^{(2)}_{AABB}$ and $g^{(1)}_{ABAB}/g^{(1)}_{AAAA}$. For $\alpha \gg 1$, the pure A channels decouple leading to

$$g^{(1)}_{AAAA}(S) = \frac{g^{(1)}_{AAAA}}{1 - 2g^{(1)}_{AAAA} \ln S} \tag{17}$$

and

$$g^{(1)}_{AAAA}(S) - 2g^{(2)}_{AAAA}(S) = C_0 = \text{initial values} . \tag{18}$$

Inserting these in the differential equations for the $AABB$ channel, one finds the solutions

$$g^{(1)}_{AABB}(S)+g^{(2)}_{AABB}(S)=(g^{(1)}_{AABB}+g^{(2)}_{AABB})\times(1-2\alpha g^{(1)}_{AAAA}\ln|S|)^{-3/4}\times|S|^{-1/2\alpha C_0}, \quad (19)$$

and

$$g^{(1)}_{AABB}(S)-g^{(2)}_{AABB}(S)=(g^{(1)}_{AABB}-g^{(2)}_{AABB})\times(1-2\alpha g^{(1)}_{AAAA}\ln|S|)^{1/4}\times|S|^{-1/2\alpha C_0}. \quad (20)$$

For $g^{(1)}_{AAAA}>0$, the important factor in both Eqs. (16) and (17) is $S^{-1/2\alpha C_0}$. For short-range couplings in the A channel ($g^{(1)}_{AAAA}=g^{(2)}_{AAAA}$), $C_0<0$. Thus both $g^{(1)}_{AABB}$ and $g^{(2)}_{AABB}$ decrease for decreasing S.

Equations (19) and (20) can be used in Eqs. (12e) and (12f) to study the behavior of the *BBBB* channel. If the initial couplings $g^{(1)}_{BBBB}=g^{(2)}_{BBBB}=0$, $g^{(2)}_{BBBB}$ tends to negative values in scaling [see Eq. (10b)], while $g^{(1)}_{BBBB}$ tends to positive or negative values depending on whether the initial coupling product $g^{(1)}_{AABB}g^{(2)}_{AABB}$ is negative or positive and both remain finite. Furthermore, the inequality, $|g^{(1)}_{BBBB}|<-g^{(2)}_{BBBB}$ holds.

Thus, a repulsive interaction in the *AAAA* channel and finite initial interactions in the *AABB* channels induce finite interaction in the *BBBB* channels. The susceptibilities due to these induced interactions can be obtained by using Eqs. (16a)—(16d). As a consequence of the inequality $|g^{(1)}_{BBBB}|<-g^{(2)}_{BBBB}=|g^{(2)}_{BBBB}|$, both the singlet and the triplet superconducting susceptibility diverge. Furthermore, the triplet superconductivity is more divergent than the singlet if the initial coupling product $g^{(1)}_{AABB}g^{(2)}_{AABB}<0$. [In the latter case, as a consequence of Eqs. (19) and (20), that product remains negative for the whole scaling region, thus, $g^{(1)}_{BBBB}>0$ as follows from Eq. (12e).] The validity of these results depends on the applicability of the large-α approximation to be discussed in the following. These results, however, show that there is a temperature region where the superconducting fluctuations are enhanced, independently of whether or not at low temperatures couplings dropped in the $\alpha\gg1$ approximation become important.

B. Numerical analysis of scaling equations

As mentioned earlier, the range of validity of the above results is confined to the high-frequency regime. A numerical analysis has therefore been performed. The range of parameters covered in this analysis is rather limited and Eqs. (12) contain more physics than is presented here.

The numerical analysis is done in two regimes.

(i) $W_B\gg W_A$ and the initial couplings are in the order $|g_{AAAA}|\gg|g_{AABB}|\approx|g_{ABAB}|\gg|g_{BBBB}|$. We will take $g^{(1)}_{AAAA}=g^{(2)}_{AAAA}$ and $g^{(1)}_{BBBB}=g^{(2)}_{BBBB}=0$ in this regime.

(ii) $W_A\approx W_B$. Here the two bands are assumed to have similar velocities, $\alpha\approx\beta\approx1$. Also, all the initial couplings are assumed to have similar values.

1. Regime (i): $W_A\ll W_B$

The *ABAB* channel which does not enter the calculations for $\alpha\gg1$ is responsible for the failure of the large-α approximation except at frequencies near W_B. From Eqs. (12g) and (12h) we gather that if the charge-fluctuation channel *AABB* were not coupled to the *ABAB* channel, its scaling properties would be identical to those of the one-component electron gas or to the single-impurity Kondo problem, where at a similar level of approximation,

$$S\frac{dJ_\perp}{dS}=2J_\perp J_z,\quad S\frac{dJ_z}{dS}=J_\perp^2,$$

where $J_\perp$ and J_z are the transverse and the longitudinal part of the exchange interaction. We recall from Eq. (11) that $\Gamma^{\perp(1)}_{ABAB}=g^{(1)}_{ABAB}$ and $\Gamma^{\parallel}_{ABAB}=g^{(1)}_{ABAB}-g^{(2)}_{ABBA}$ to see the complete mapping of the *uncoupled ABAB* channel to the single-impurity Kondo problem. Therefore, if we start out with the exchange interaction $g^{(1)}_{ABAB}<0$, the scaling is to strong coupling. This behavior is obtained in our numerical results because the coupling to the *AABB* channel becomes unimportant except at ω close to W_B, because these couplings rapidly go towards zero.

Most of our analysis has been done with $g^{(1)}_{AABB}=g^{(2)}_{AABB}$ and $g^{(1)}_{ABAB}=g^{(2)}_{ABBA}$. Figure 5 shows the results when these couplings are all initially positive. Similar results are obtained when the *AABB* couplings are initially negative but the *ABAB* couplings are still positive. Scaling to weak coupling results and the calculations in the large-α approximation above are valid.

In Fig. 6, we show the result for initial couplings $g^{(1)}_{ABAB}=g^{(2)}_{ABBA}<0$. They both scale to $-\infty$ with $g^{(1)}_{ABAB}\approx2g^{(2)}_{ABBA}$, as required by (13b). The initial behavior shown in Fig. 6 is not changed by changing initial $|g^{(1)}_{AABB}|=|g^{(2)}_{AABB}|$, which together with the *AAAA* channel (for $g^{(1)}_{AAAA}=g^{(2)}_{AAAA}$) scale $\to0$, while the *BBBB* channel starting from an initial value 0 scales towards small negative values.

The above results are very revealing. They show that even for the complicated problem being considered, scaling for $g^{(1)}_{AAAA}=g^{(2)}_{AAAA}$, $g^{(1)}_{BBBB}=g^{(2)}_{BBBB}$, is governed by the physics of the Kondo problem. For positive initial *ABAB* couplings, scaling is to the weak-coupling fixed point, just like the one-dimensional electron gas for the prescribed *AAAA* and *BBBB* interactions and like the ferromagnetic

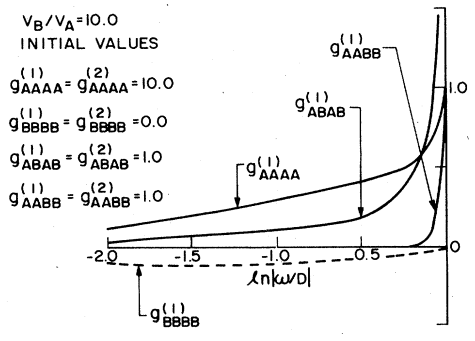

FIG. 5. Scaling of the vertices obtained by a numerical solution of Eqs. (12) with initial parameters indicated in the figure. D is the frequency cutoff $\approx W_B$. With positive *ABAB* coupling and short-range repulsive parameters in the *AAAA* channel; all the vertices scale to weak coupling.

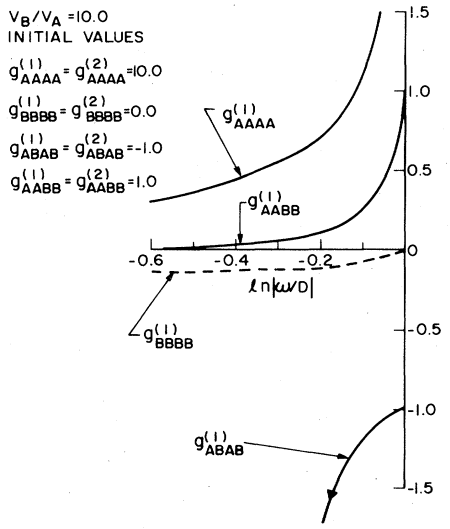

FIG. 6. Same as Fig. 5 but with attractive *ABAB* coupling; *ABAB* vertices now scale to strong coupling, unaffected by the coupling of this channel to the rest. The instability of the *ABAB* channel is likely to have interesting consequences in the *AAAA* channel in the higher-order scaling corrections.

Kondo problem. For negative initial *ABAB* couplings, scaling of the *ABAB* channel is towards strong coupling just like the antiferromagnetic Kondo problem. This behavior is unaffected by the coupling to the charge-fluctuation channel and through it to the *AAAA* and the *BBBB* channels. In the lowest-order logarithmic approximation, the instability of the *ABAB* channel does not affect the other channels. It is likely to do so in higher order. The instability in the *ABAB* channel suggests that the ground state must be reorganized. It is possible that just as in the Kondo problem there is no phase transition at a finite temperature.

The study of the susceptibilities in the *AB* channel may help to understand the meaning of the divergencies in the *ABAB* channel. Using Eqs. (16a)—(16d) one can see that for $g^{(1)}_{ABAB} \approx 2g^{(2)}_{ABBA} \to -\infty$ the singlet superconducting and the Peierls susceptibilities diverge with the same strength. The superconducting susceptibility indicates the formation of singlets consisting of an *A* and *B* electron, and the Peierls instability corresponds to the formation of a pair from, e.g., an *A*-electron and *B*-hole. These singlet formations show strong resemblance to the formation of Kondo singlets.

It is suggested by these calculations that the physics, in the frequency regime being discussed, is related to the Kondo problem. This should be considered alongside the fact from the theoretical side, that the single fluctuating-valence impurity and the Kondo impurity problems are known to have the same ground state and low-lying excitations. On the phenomenological side, the fluctuating-valence solids have a Fermi-liquid behavior qualitatively similar to the so-called heavy-fermion solids where the charge fluctuations are negligible.

A word of caution is necessary about the passage of the *AABB* couplings to zero under scaling. The *AABB* coupling undoubtedly rapidly decreases initially, as shown in Fig. 6. However if we take *ABAB* couplings near their asymptotic large negative value with $g^{(1)}_{ABAB} = 2g^{(2)}_{ABAB}$, and ignore the *AAAA* and *BBBB* channels in examining the behavior of the *AABB* channel, the conclusion is that $|g^{(1)}_{AABB}|$ tends to become very large. This is seen through Eqs. (12a) and (12b). If we feed this back into Eqs. (12g) and (12h) for the *ABAB* couplings, the behavior is unchanged from that discussed above. The growth of the *AABB* channel, if it happens, is at too low a frequency to conveniently analyze numerically. Moreover, the leading-order scaling is dubious for an analysis of such a reversal in behavior from that found initially.

For $g^{(1)}_{AAAA} \approx 2g^{(2)}_{AAAA} > 0$, the *ABAB* can induce instabilities in the *AAAA* channel depending on the starting values in the *AABB* channel. The behavior is rather complicated and we do not pursue it in this paper.

2. *Regime (ii): $W_A \approx W_B$*

As a matter of general interest, we have done a limited numerical analysis in this regime. We have taken $v_A/v_B = 1$, and $g^{(1)}_{AAAA} = g^{(2)}_{AAAA} = g^{(1)}_{BBBB} = g^{(2)}_{BBBB} > 0$, and $g^{(1)}_{ABAB} = g^{(2)}_{ABBA}$, $g^{(1)}_{AABB} = g^{(2)}_{BBBB}$. For positive *ABAB* and *AABB* channels, the scaling is to weak coupling if the *AABB* and *ABAB* couplings are both much less than the *AAAA* and *BBBB* couplings. When this is not satisfied, scaling is towards weak coupling for $g^{(1)}_{AABB} \lesssim g^{(1)}_{ABAB}$ and to strong coupling for $g^{(1)}_{AABB} \gtrsim g^{(1)}_{ABAB}$. This behavior is illustrated in Fig. 7.

For negative initial couplings in the *ABAB* channel, behavior similar to that discussed in regime (i) is found for the *ABAB* channel, accompanied by a divergent behavior in the *AABB* channel towards $+\infty$ as the frequency scale is decreased. This in turn leads to divergent behavior in the *AAAA* and *BBBB* channels.

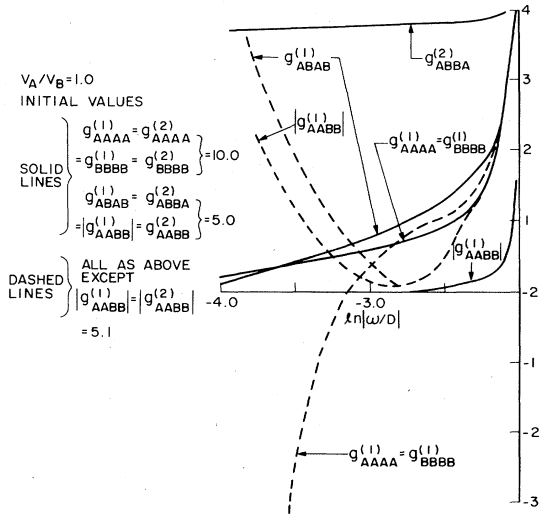

FIG. 7. Scaling for $|\omega| < W_A$. In this figure, $D \approx W_A$. Results for two sets of initial parameters are shown and discussed in the text.

V. SUMMARY

We have derived the leading-order scaling equations for the two-component one-dimensional electron gas. The limited range of parameters for which these equations have been analyzed corresponds to a fluctuating-valence problem. It is discovered that the renormalization-group flows are determined by the exchange interactions (*ABAB* channel) between the two components and that the charge-fluctuation interactions (*AABB* channel) do not determine the strongest instabilities. It would appear that the ground state and low-lying excitations of the fluctuating-valence state, provided it is not semiconducting, are of the same nature as a model without charge fluctuations in one of the components, such as the so-called Kondo lattice model. This would appear to be true, also phenomenologically.

The instabilities in the *ABAB* channel are likely to lead in the next-order scaling to important self-energy corrections and instabilities in the various other channels. This would be well worth pursuing. But if, as we suspect, for an interesting range of parameters, the scaling is to strong coupling, the present methods are inadequate for a complete treatment. The knowledge of the manner of approach to strong coupling acquired by these methods is however essential.

Finally, we must remark that the present calculations are justified only in the weak-coupling limit, but the Monte Carlo calculations[11] in the single-band models show that the first-order scaling equations give correct results even in the intermediate- and strong-coupling regions. Thus, the applicability of the results obtained in the present paper is likely to be beyond the weak-coupling region, at least, in a qualitative sense.

ACKNOWLEDGMENTS

One of the authors, A. Z., must express his gratitude to V. Emery, E. Abrahams, and H. Bilz for their hospitality and valuable discussions at Brookhaven National Laboratories, Rutgers University, and the Max Planck Institute in Stuttgart, Germany. C. M. V. is also grateful to E. Abrahams for several discussions. This work has been partially supported by DE-AC02-76CH00016 and by the NSF under Grant No. DMR-82-16223.

[1]J. Sólyom, Adv. Phys. **28**, 201 (1979).

[2]C. M. Varma, Rev. Mod. Phys. **48**, 219 (1976); J. M. Lawrence, P. S. Riseborough, and R. D. Parks, Rep. Prog. Phys. **44**, 1 (1981).

[3]B. Batlogg, H. R. Ott, and P. Wachter, Phys. Rev. Lett. **42**, 282 (1979).

[4]C. M. Varma, Solid State Commun. **30**, 537 (1979).

[5]For a review of the experimental properties, see G. R. Stewart, Rev. Mod. Phys. **56**, 755 (1984).

[6]For a review of the theoretical situation, see C. M. Varma, Comments Solid State Phys. **11**, 221 (1985).

[7]C. M. Varma and Y. Yafet, Phys. Rev. B **13**, 295 (1975); A. Bringer and H. Lustfeldt, Z. Phys. B **28**, 213 (1977); F. D. Haldane, Phys. Rev. Lett. **40**, 416 (1978); H. R. Krishnamurthy, K. G. Wilson, and J. W. Wilkins, Phys. Rev. B **21**, 1003 (1980).

[8]C. Jayprakash, H. R. Krishnamurthy, and J. W. Wilkins, J. Appl. Phys. **53**, 2143 (1982); C. M. Varma, in *Moment Formation in Solids,* edited by W. J. Buyers (Plenum, New York, 1984).

[9]K. G. Wilson, Rev. Mod. Phys. **47**, 773 (1975); P. Nozières, J. Low Temp. Phys. **17**, 31 (1974).

[10]N. Menyhárd and J. Sólyom, J. Low Temp. Phys. **12**, 529 (1973).

[11]J. E. Hirsch and D. J. Scalapino, Phys. Rev. B **27**, 7169 (1983).